2019 Conference
S E C E D
Earthquake risk and engineering
towards a resilient world

9-10 September 2019, Greenwich, London

PROBABILISTIC SEISMIC HAZARD ANALYSIS OF A CO$_2$ STORAGE PROSPECT USING THE NGA EAST GROUND MOTION MODELS

Brian CARLTON[1], Elin SKURTVEIT[2], Kuvvet ATAKAN[3] & Amir M. KAYNIA[4]

Abstract: *The Smeaheia fault block in the North Sea is a site under consideration for large scale CO$_2$ storage. Even though the overall earthquake hazard in the North Sea is low, it is necessary to evaluate the risk related to earthquake hazard at the site to ensure safe storage of CO$_2$ and to provide a baseline to be able to estimate the change in earthquake hazard due to future CO$_2$ injection. This paper presents a probabilistic seismic hazard analysis (PSHA) for Smeaheia using an updated earthquake catalogue, two alternate source models and the final NGA East ground motion models. Defining the specific hazard related to the Vette and Øygarden faults, which bound the site, was not feasible due to a lack of data and uncertainty in earthquake location. However, by characterizing the main fault defining the continental-oceanic crust transition as an areal source zone, the results show that this zone dominates the earthquake hazard for the site. The results also show that the main earthquake scenarios that contribute to the hazard are magnitude 5 to 6 earthquakes 20 to 120 km from the site. The calculated peak ground accelerations (PGA) for 475 year and 2475 year return periods are 0.031 g and 0.088 g, respectively, which are smaller than in past studies.*

Introduction

A promising solution to reduce carbon dioxide (CO$_2$) emissions to the atmosphere is sequestration in geologic formations. Researchers at the Norwegian Carbon Capture and Storage Research Centre (NCCS) have identified Smeaheia on the Norwegian continental shelf as a potential storage site. The Smeaheia site is located on the Horda Platform east of the Troll field in the North Sea, roughly 60 km northwest from the city of Bergen, Norway (Figure 1). The reservoir is within a fault block with Upper Jurassic Sognefjord sandstone bounded by the Vette fault to the West and Øygarden fault complex (ØFC) to the East (Skurtveit et al., 2018).

To ensure safe storage of CO$_2$ and to be able to evaluate the change in earthquake hazard due to future CO$_2$ injection, the current earthquake hazard at the site needs to be defined. However, the only publically available seismic hazard studies that include the project site are Bungum et al. (1998) and Bungum et al. (2000), which are both based on data and methodologies from 20 years ago. Since then, there have been considerable advances in seismic hazard assessment techniques and the earthquake catalogue is significantly enlarged, with several reinterpretations of important historical earthquakes. Other seismic hazard studies of nearby onshore locations include Gruenthal et al. (1999), Wahlstrom and Gruenthal (2001), and Woessner et al. (2015). However, these studies are for large regions with coarse interpretations that are not as accurate as site specific studies.

In this study we present a site specific probabilistic seismic hazard analysis (PSHA) for the Smeaheia site. We use an earthquake catalogue updated through to 2018, incorporate two alternative source models, and use the final NGA East ground motion models (Goulet et al., 2018), which specifically address the epistemic uncertainty for stable continental regions. The following section discusses the tectonic setting and local seismicity. We then describe the PSHA methodology, present the results, and compare the results with the studies listed above.

---

[1] Norwegian Geotechnical Institute (NGI), Oslo, Norway, brian.carlton@ngi.no
[2] NGI and University of Oslo, Oslo, Norway
[3] University of Bergen, Bergen, Norway
[4] NGI and Norwegian University of Science and Technology, Trondheim, Norway

Background

Tectonic setting

The Smeaheia site is located in a fault block on the Horda Platform on the eastern margin of the Northern North Sea Viking Graben structure. The fault block is bounded to the east by the north-south trending Øygarden Fault Complex, a major rift fault (Figure 1). To the west, the Vette fault separates Smeaheia from the Troll East gas field. Approximately north-south trending faults are the main structural elements formed during the rifting, however, several pre-rift Devonian shear zones were re-activated during the rifting and are believed to influence the rift system by offsetting, terminating or bending the rift related faults as they approach the low angle shear zones (Fossen et al., 2017).

The North Sea rift system may be divided into several episodes as summarized in Gabrielsen et al. (2015) and Fossen et al. (2017). A late Caledonian extension and gravitational collapse activated the low angle normal shear zones. As displacement accumulated, the extension was taken up by new and steeper shear zones like the Nordfjord-Sogn detachment (NSDZ), Bergen Arch Shear Zone (BASZ), Hardangerfjord Shear Zone (HSZ), Karmøy shear zone (KSZ) and Stavanger shear zone (SSZ), which are marked on Figure 1. This was followed by Permian to Early Triassic rifting (stretching) and later Triassic to early Jurassic post-rift subsidence. A second rifting occurred in the mid to late Jurassic and was accompanied with post-rift subsidence. In the Jurassic-Cretaceous, development of the Viking Graben re-activated most of the structures.
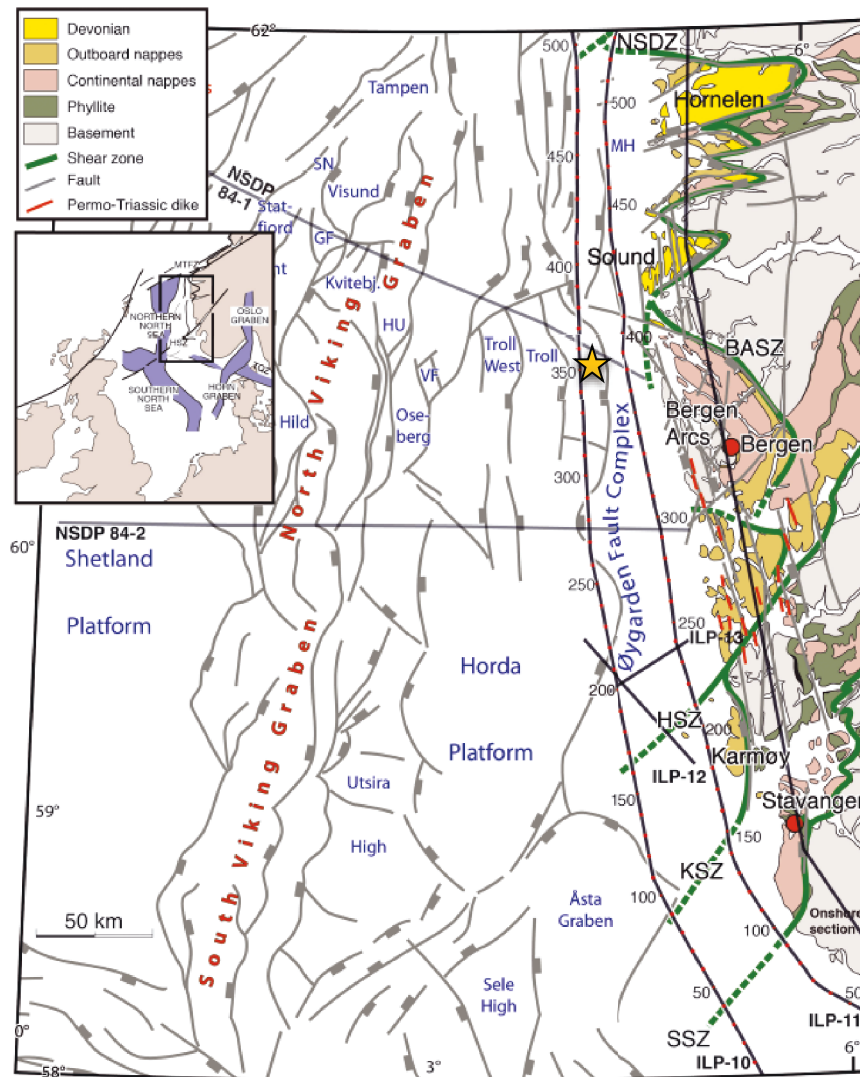

Figure 1. Structural map of the Norwegian west coast and the offshore Viking Graben rift system from Gabrielsen et al. (2015). Smeaheia site marked with star.

The North-South trending Øygarden Fault Complex (ØFC) represents a major structural divide between the eastern Precambrian and lower Palaeozoic rocks of mainland Norway and the western side where the basement rock is found at depths up to 8-10 km (Figure 1). The ØFC also marks a sharp transition in crustal thickness from the mainland to the thinned Horda Platform within the North Sea sedimentary basin. Permian to Early Triassic rifting is well exposed on the Horda Platform and involved the ØFC. The ØFC was also reactivated in the Mid-late Jurassic rifting. The main extensional event took place in the mid-Permian to early Triassic stretching event where throws up to 3-5 km on individual faults can be observed (Færseth et al., 1995), whereas only minor displacements (<300 m) took place in the late Jurassic to early Cretaceous time.

The ØFC polarity is mainly dipping to the west, however, a subsidiary system of polarity with dip to the east is also observed and related to the shear zones in the basement. The present fault dip varies from 30°-35° in the basement to 40°-50° in the upper sedimentary succession (Færseth et al., 1995). The Vette fault, the western margin of Smeaheia, is considered a subsidiary fault relative to the ØFC. It is related to the basin horst and graben structure, but seismic data also shows a link to more deep-seated structures.

Local seismicity

Western Norway has higher seismicity than the rest of Norway, however, the seismicity is still relatively low. Figure 2 shows earthquakes within a 250 km radius around the site. The largest known earthquake in the study area is a M_w = 5.0 that occurred in 1927 about 160 km to the south-west of the site. The data is from the Norwegian National Seismic Network (NNSN), which is operated by the University of Bergen. The NNSN began in the early 1980's, however the first seismograph station in Norway was installed in 1905, and reliable accounts of felt earthquakes date back to the 1700's.

The locations of earthquakes in the study area have uncertainties up to ±10 km, with even more uncertainty in the depth estimates. This is especially true for the smaller magnitude earthquakes that occur offshore. As a result, assigning earthquake events to mapped faults is difficult due to the low seismic resolution and high uncertainty in the location of the seismic events. However, the seismic activity can be correlated with the main tectonic elements on a regional level. Two clusters of earthquakes can be observed in Western Norway (Figure 3), one to the north-east of the site that may be related to the Nordfjord-Sogn detachment and the other cluster a possible magnetic anomaly south of Bergen.

PSHA methodology

Source identification

We used two different models to describe the earthquake sources: (1) a model where the area is divided into regions based on the geological characteristics and (2) a model with smoothed gridded seismicity for the entire area. The first model consists of three areal source zones: an ocean source zone representing oceanic crust and the offshore sediment basin, a continental source zone representing the Norwegian basement rock on the continental crust, and a fault source zone representing the transition zone that is characterized by a series of faults and discontinuities (Figure 2). The second model consists of one areal source zone over the entire area with smoothed gridded seismicity (Figure 3). Smoothed gridded seismicity is a grid of very small areal sources with different relative activity rates but the same magnitude probability density function and b-value. The different relative activity rates represent the spatial variability of earthquake occurrence. The relative rates of each cell are based not just on the earthquakes that occurred in that cell, but a weighted average of the rates of the cell and the cells around it. We used a Gaussian distribution with a 30 kilometre radius and 0.1° by 0.1° grid cells to calculate the smoothed gridded seismicity. Figure 3 shows the relative activity rates of the gridded seismicity. In this model, there are two main hotspots of earthquake activity occurring to the north and the southeast of the site.

We incorporated both models in the analysis using a logic tree framework, giving equal weight to each model.
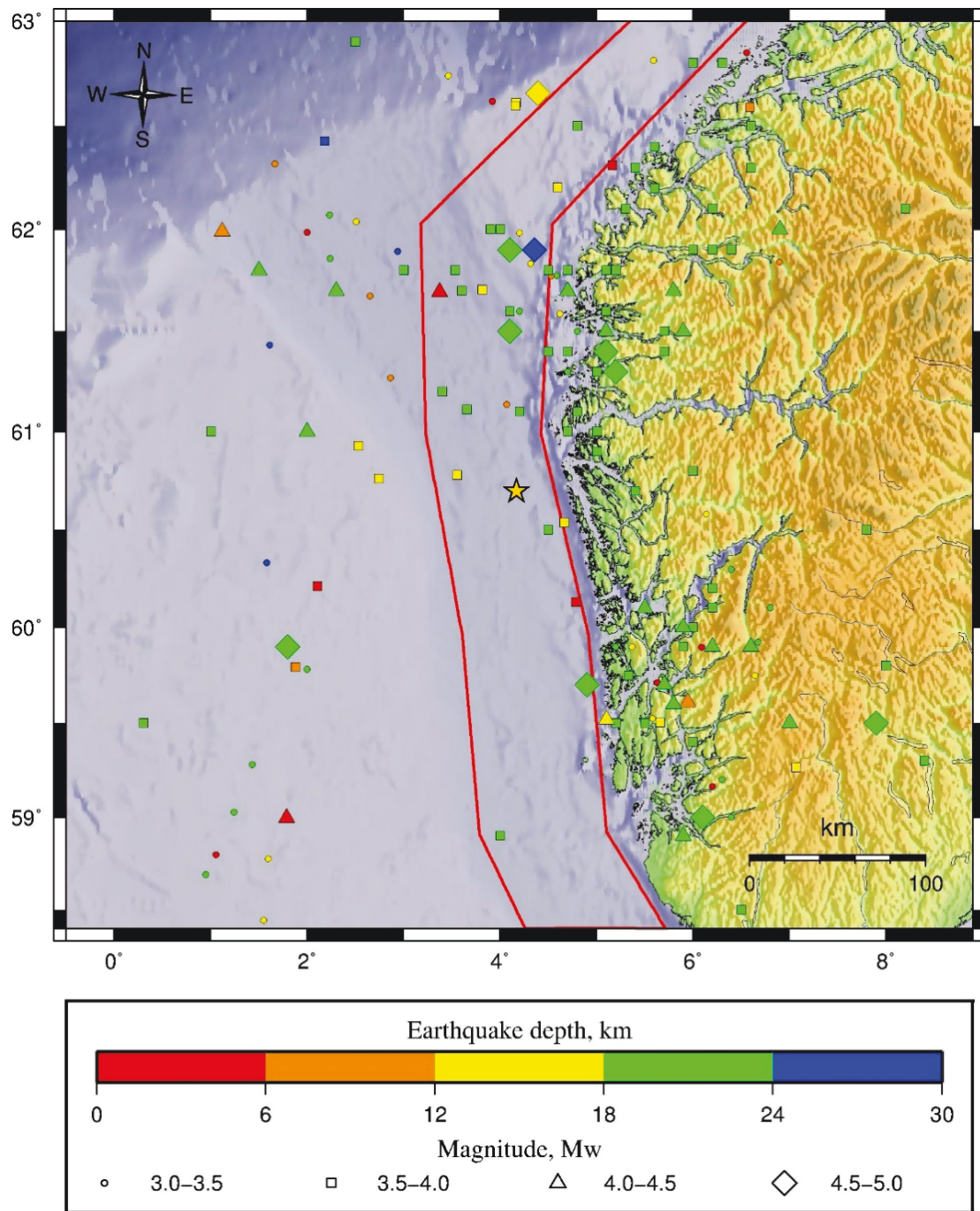
Figure 2. Earthquake locations and source model 1. The red lines define the source boundaries, and the yellow star shows the site location. The left zone is the Ocean source, the middle is the Fault Zone source, and the right zone is the Continental source.

Magnitude recurrence relations

We modelled all four sources using the truncated exponential model, which is based on the Gutenberg-Richter relation (Gutenberg and Richter, 1944), but modified to include a minimum magnitude (M_{min}) and a maximum magnitude (M_{max}). The truncated exponential model works well for areal source zones that implicitly include a wide range of fault lengths, however, it is not suitable for specific faults (Youngs and Coppersmith, 1985).

We estimated the necessary parameters for the truncated exponential model from the NNSN earthquake catalogue, which includes both recorded and historical earthquakes for Norway. We used the correlations proposed by Bungum et al. (1998) to convert the earthquake events in the catalogue to moment magnitude. We then removed the dependent events using the declustering model of Gruenthal (1985) and estimated the completeness for different magnitude bins following

the method of Stepp (1972). Finally, we calculated the activity rate and b-value of the truncated exponential model using the maximum likelihood method of Weichert (1980). Figure 4 compares the calculated values (solid lines) to the catalogue data (boxes) for different earthquake magnitude bins. The error bars show the 5 to 95 percentile of the uncertainty.

Table 1 lists the activity rates, b-values, M_{min} and M_{max} values used in the PSHA for each source. Table 1 shows that all four sources have similar b-values around 1.2, but with different activity rates (a). We used M_{min} values of 4.0 because the ground motion models are defined down to M_w = 4.0. However, we used earthquakes down to M_w = 3.5 to help constrain the b-values (Figure 4). We did not use earthquakes with M_w < 3.5 to constrain the b-values as they were incomplete.

The M_{max} values for the Fault zone are 7.0, which is the maximum magnitude recommended by (Bungum et al., 1998) for Norway, and 6.5. The M_{max} values for the other two zones are conservatively set at 6.0 and 6.5. For the areal source zone over the entire area (Background) we used a combination of the M_{max} values from all of the other zones.
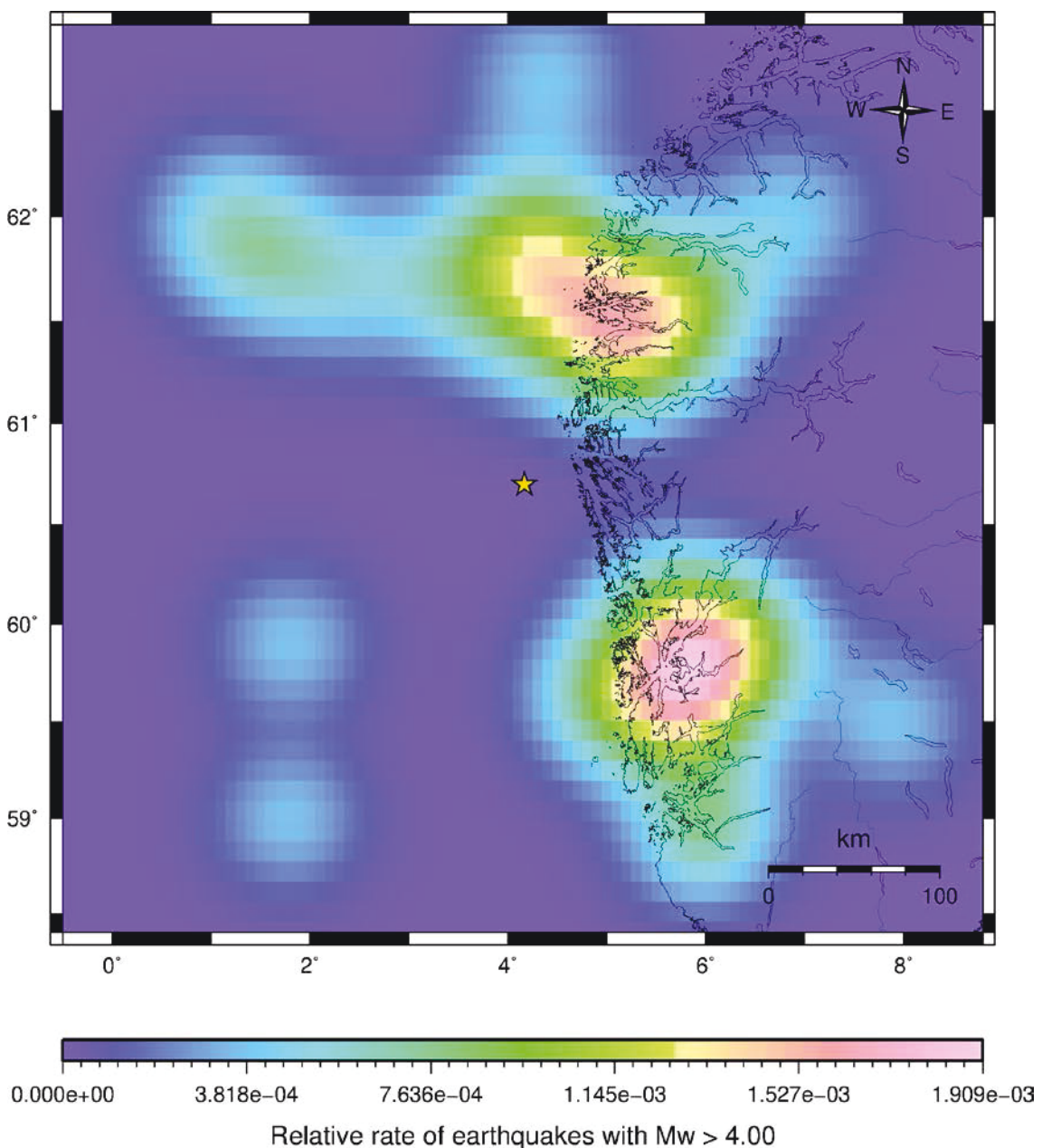

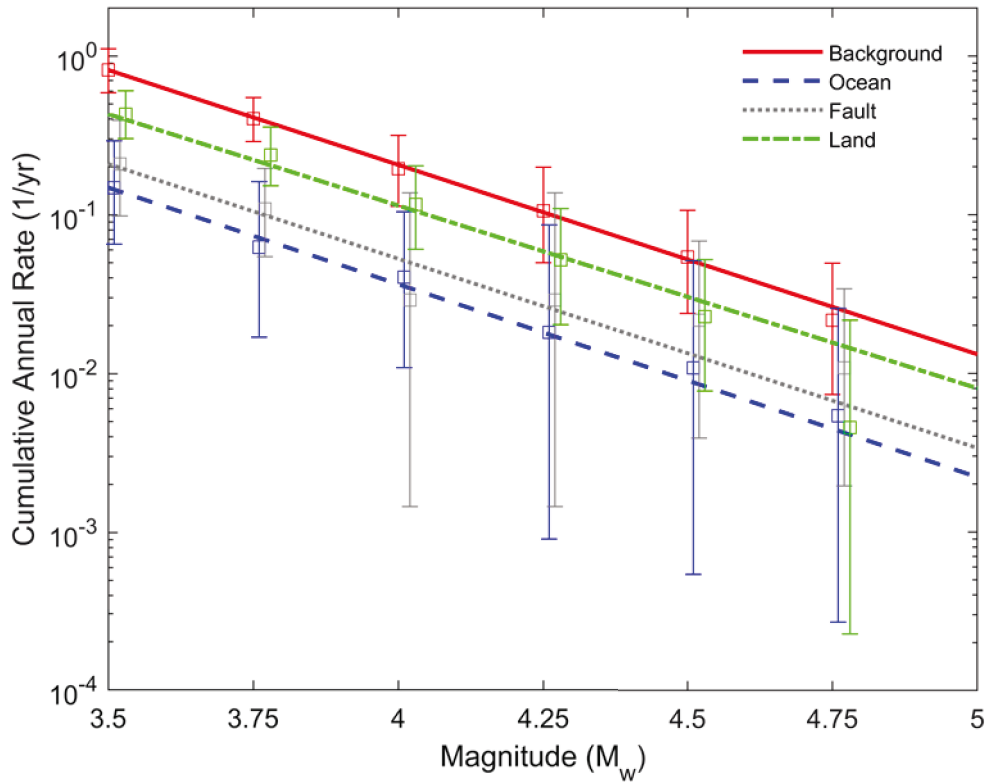*Figure 3. Smoothed seismicity heat map and source model 2 (Background source).*

Figure 4. Magnitude recurrence relations versus cumulative annual rates.

Source	a	b	M_{min}	M_{max}
Background	0.2063	1.20	4.0	6.0, 6.5, 7.0
Ocean	0.0365	1.22	4.0	6.0, 6.5
Fault	0.0528	1.19	4.0	6.5, 7.0
Land	0.1142	1.15	4.0	6.0, 6.5

Table 1. Magnitude recurrence parameters

Ground motion models

We used the final NGA East median ground motion models with the composite ergodic sigma standard deviation model (Goulet et al., 2018). These models were developed for central and eastern North America, which is a stable continental region similar to the North Sea. The models are valid for periods from 0.01 to 10 seconds, M_w = 4 to 8.2, and rupture distances of 0 to 1500 km. The models require the moment magnitude and rupture distance as inputs, and are defined for Vs_{30} = 3,000 m/s. We used the period and model dependent weights specified in Goulet et al. (2018) in a logic tree framework to capture the epistemic uncertainty. The 17 different median models, the standard deviation models, and their weights represent the "ground motions' center, body, and range of the technically defensible interpretations in light of the available data and models" (Goulet et al., 2018). We did not include the adjustment factors for source-depth effects, hanging-wall effects, or the Gulf Coast region.

Results and discussion

Figure 5 shows the hazard curve for the PGA and spectral periods from 0.02 seconds to 10 seconds. Figure 6 shows the hazard curve for PGA by source. For return periods less than 300 years the Background zone contributes the most to the hazard because it has the largest activity rate. For return periods greater than 300 years the Fault zone contributes the most because it is the closest to the site. The contributions of the Land and Ocean sources to the hazard are insignificant.
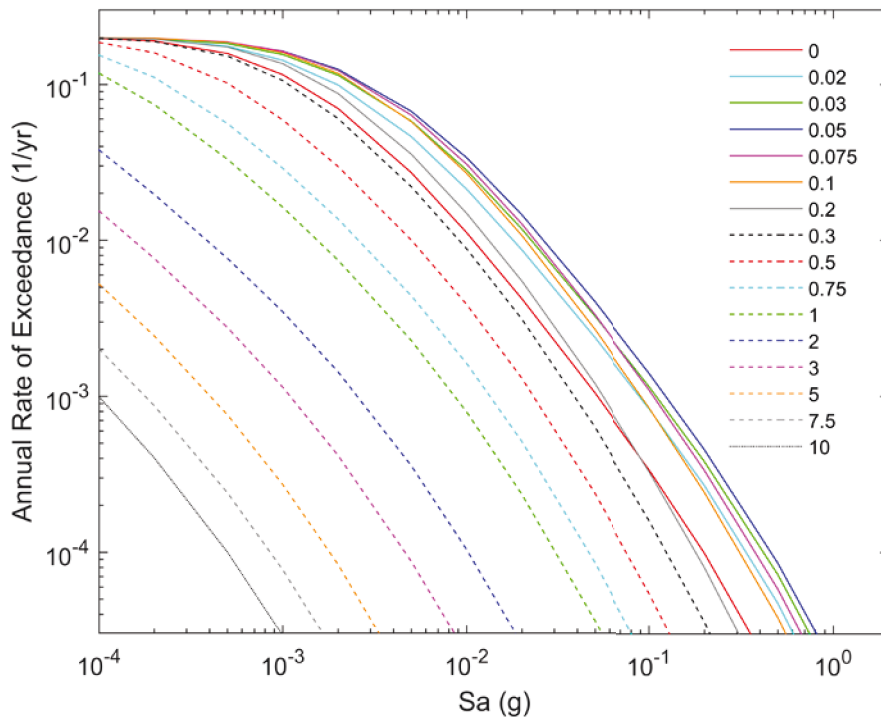
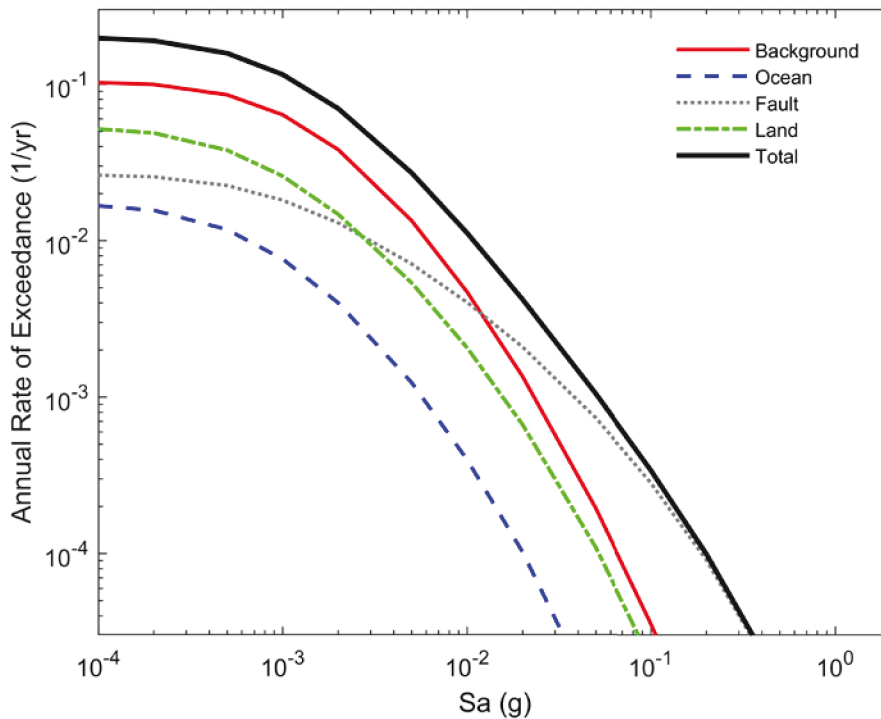*Figure 5. Mean hazard curves on rock for PGA (0 s) and periods from 0.02 to 10 seconds*

Figure 6. Hazard curves by source for PGA on rock

Figure 7 presents magnitude and distance deaggregation plots for PGA and a spectral period of 1 second (Sa(T=1)) for a return period of 475 years. The deaggregation plots shows the relative contribution to the hazard for a given magnitude and distance bin. Figure 7 shows that the modal earthquake scenario, i.e. the single scenario that most contributes to the hazard, is a magnitude 4.0 – 4.5 with distance 10 – 20 km from the site for PGA, and magnitude 5.5 – 6.0 with distance 150 – 200 km from the site for Sa(T=1). Figure 8 shows the mean magnitude and distance of the deaggregation for four return periods and all spectral periods. Figure 8 shows that for short periods, nearby small magnitude earthquakes dominate the hazard, whereas for long periods distant large magnitude earthquakes dominate the hazard.
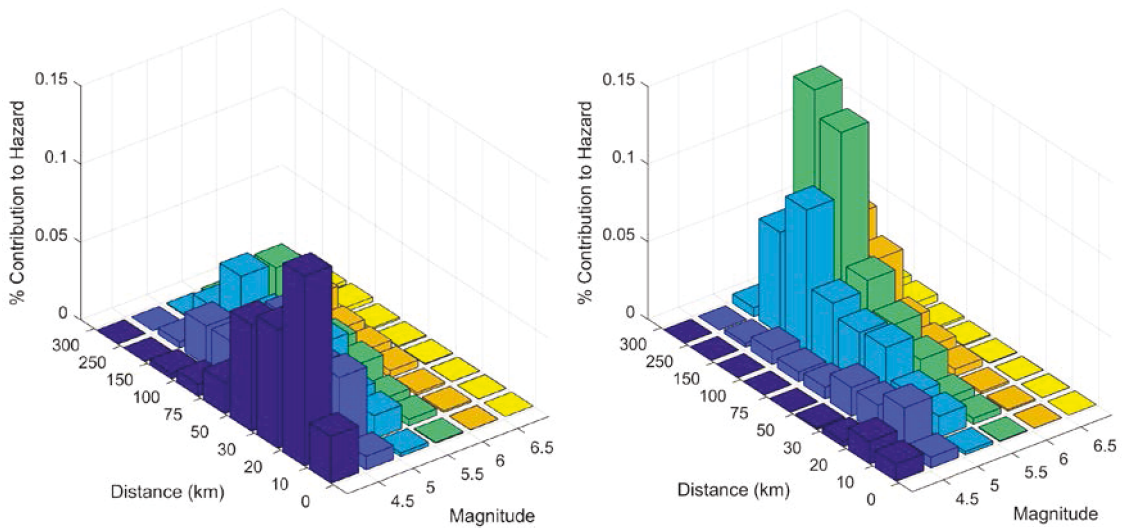
Figure 7. Deaggregation plot for PGA (left) and spectral acceleration at one second (right) on rock for a return period of 475 years
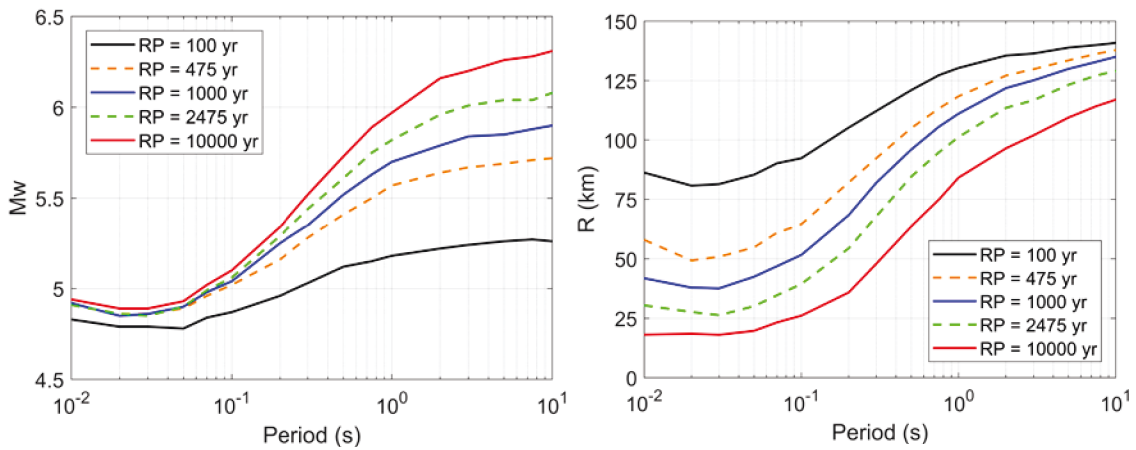

Figure 8. Mean magnitude (left) and distance (right) of the deaggregation

Figure 9 shows the uniform hazard spectra (UHS) for return periods of 100, 475, 1000, 2475, and 10000 years. In general, the UHS for 2475 years is about 3 times larger than for 475 years.

Comparison with other studies

Table 2 compares the peak ground acceleration values on rock for return periods of 475 years and 2475 years calculated in this study with five other studies. The other studies are for sites with Vs_{30} = 760 to 800 m/s, whereas the NGA East models are for Vs_{30} = 3,000 m/s. However, for PGA, the site amplification factor from Vs_{30} = 3,000 to 760 m/s is about 1.0 (PEER, 2015), therefore, the comparison is still valid. Only the Bungum et al. (1998) study includes values for offshore. For the other studies, we have listed the values for the closest points on land. Table 2 shows that the results of this study are lower than the results of the other studies. This could be due to the different ground motion models used, the different earthquake catalogues, magnitude conversion models, and/or declustering methods. The NGA East models were developed after the other studies were completed and include a more thorough treatment of epistemic uncertainty. In addition, in low seismicity areas with few recorded earthquakes such as western Norway, even a few small differences in the estimated magnitudes, quantity, and locations of earthquakes can affect the results. Therefore, we believe the results from the present study are more accurate and realistic than those considered in the comparison.
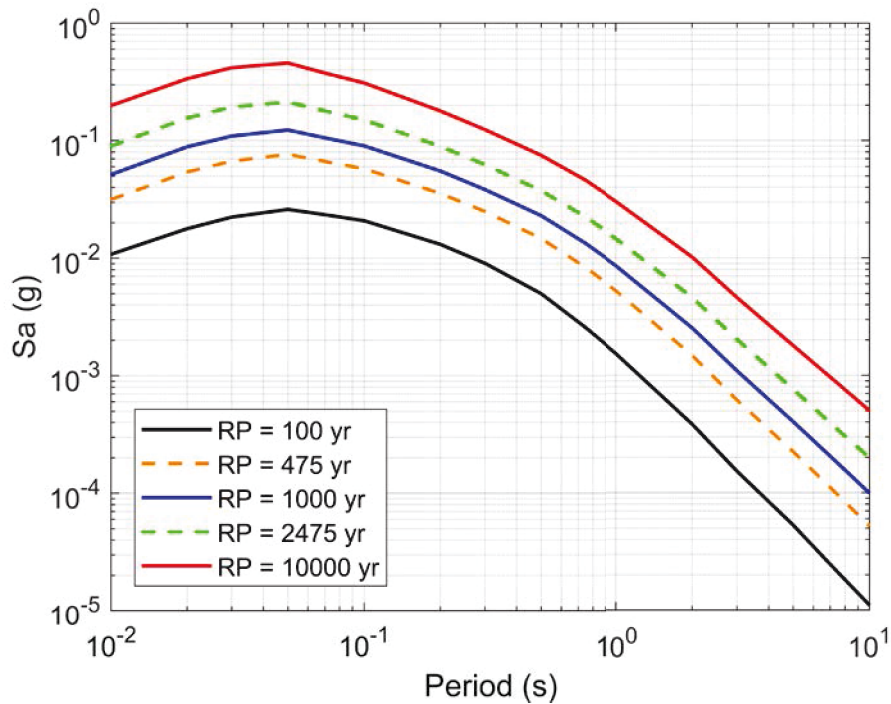
Figure 9. Uniform Hazard Spectra for four return periods on rock

Reference	475 yr	2475 yr
This study (2019)	0.31	0.88
Woessner et al. (2015) (SHARE)	0.5-0.7	1.5-2.0
Wahlstrom and Gruenthal (2001)	0.5-0.7	1.5
Bungum et al. (2000)	0.6-1.0	2.1
Gruenthal et al. (1999) (GSHAP)	0.8-1.0	
Bungum et al. (1998)	0.64-0.8	

Table 2. Comparison of PGA values on rock in m/s^2 for two return periods.

Conclusions

This paper presented a probabilistic seismic hazard analysis for a potential future carbon sequestration site located in the North Sea. Due to the lack of data and the uncertainty in earthquake locations in the North Sea, it was not feasible to define specific faults. Therefore, we used a source model that consists of two sub-models, one with three areal source zones and the other with one areal source zone using smoothed gridded seismicity. In addition, we used the NGA East median ground motion models with the composite ergodic sigma standard deviation model (Goulet et al., 2018). The results show that the earthquake hazard is dominated by magnitude 5 - 6 earthquakes 20 – 120 km from the site in the Fault zone source. The PGA values of this study are lower when compared with past studies. This is most likely due to the use of different ground motion and source models. The NGA East models were developed after all of the other studies were finished. In addition, the other studies are all large regional studies, with coarser interpretations of seismic sources than possible in site specific studies. Therefore, we believe the results from the present study provide a more accurate prediction of the earthquake hazard at the Smeaheia site, which will ensure safe storage of CO_2. In addition, the results of this study will provide a baseline that will help evaluate the change in the earthquake hazard due to future CO_2 injection.

Acknowledgements

Energia, CoorsTek Membrane Sciences, Equinor, EMGS, Gassco, KROHNE, Larvik Shipping, Norcem, Norwegian Oil and Gas, Quad Geometrics, Shell, TOTAL, and the Research Council of Norway (257579/E20).

References

Bungum H, Lindholm C, Dahle A, Hicks E, Høgden S, Nadim F, Holme J, and Harbitz C (1998), Development of a seismic zonation for Norway, Final report.

Bungum H, Lindholm C, Dahle A, Woo G, Nadim F, Holme J, Gudmestad O, Hagberg T, and Karthigeyan K (2000), New seismic zoning maps for Norway, the North Sea, and the United Kingdom, *Seismological Research Letters*, 71(6): 687-697.

Fossen H, Khani HF, Faleide JI, Ksienzyk AK, and Dunlap WJ (2017), Post-Caledonian extension in the West Norway–northern North Sea region: the role of structural inheritance, Geological Society, London, Special Publications, 439(1): 465-486.

Færseth RB, Gabrielsen RH, and Hurich CA (1995), Influence of basement in structuring of the North Sea basin, offshore southwest Norway, *Norsk Geologisk Tidsskrift*, 75(2-3): 105-119.

Gabrielsen RH, Fossen H, Faleide JI, and Hurich CA (2015), Mega-scale Moho relief and the structure of the lithosphere on the eastern flank of the Viking Graben, offshore southwestern Norway, *Tectonics*, 34(5): 803-819.

Goulet C, Bozorgnia Y, Abrahamson N, Kuehn N, Al Atik L, Youngs R, Graves R, Atkinson G (2018), Central and Eastern North America Ground-Motion Characterization: NGA-East Final Report, Pacific Earthquake Engineering Research Center, Berkeley, CA. PEER Report No. 2018/08.

Gruenthal, G, and the GSHAP Region 3 Working Group, (1999), Seismic hazard assessment for central, north and northwest Europe: GSHAP Region 3, *Annals of Geophysics*, 42(6)

Gruenthal, G (1985), The up-dated earthquake catalogue for the German democratic Republic and adjacent areas–statistical data characteristics and conclusions for hazard assessment, in Proceedings Proc. 3rd Int. Symp. on the Analysis of Seismicity and Seismic Risk. Liblice, Czechoslovakia.

Gutenberg, B, and Richter, CF (1944), Frequency of earthquakes in California, *Bulletin of the Seismological Society of America*, 34(4): 185-188.

PEER, 2015. NGA-East: Median Ground-Motion Models for the Central and Eastern North America Region. Pacific Earthquake Engineering Research Center, Berkeley, CA. PEER Report No. 2015/04.

Skurtveit, E, Choi, JC, Mulrooney M, Osmond JL, and Braathen A (2018), 3D fault integrity screening for Smeaheia CO2 injection site.

Stepp, J (1972), Analysis of completeness of the earthquake sample in the Puget Sound area and its effect on statistical estimates of earthquake hazard, in Proceedings Proc. of the 1st Int. Conf. on Microzonazion, Seattle, 2: 897-910.

Wahlstrom, R., and Gruenthal, G. (2001), Probabilistic seismic hazard assessment (horizontal PGA) for Fennoscandia using the logic tree approach for regionalization and nonregionalization models, *Seismological Research Letters*, 72(1): 33-45.

Weichert DH (1980), Estimation of the earthquake recurrence parameters for unequal observation periods for different magnitudes, *Bulletin of the Seismological Society of America*, 70(4): 1337-1346.

Woessner J, Laurentiu D, Giardini D, Crowley H, Cotton F, Grünthal G, Valensise G, Arvidsson R, Basili R, and Demircioglu MB (2015), The 2013 European seismic hazard model: key components and results, *Bulletin of Earthquake Engineering*, 13(12): 3553-3596.

Youngs, RR, and Coppersmith KJ (1985), Implications of fault slip rates and earthquake recurrence models to probabilistic seismic hazard estimates, *Bulletin of the Seismological society of America*, 75(4): 939-964.